Far-infrared study of localized states in In-doped $Pb_{0.75}Sn_{0.25}Te$ single crystals

N. Romčević and Z. V. Popović
Institute of Physics, P. O. Box 57, 11001 Belgrade, Yugoslavia

D. Khokhlov
Low-Temperature Physics Department, Moscow State University, 117234 Moscow, U.S.S.R.

A. V. Nikorich
Applied Physics Institute of the Moldavian Academy of Science, Kishenev, U.S.S.R.

W. König
Max-Planck-Institut für Festkörperforschung, Heisenbergstrasse 1, 7000 Stuttgart 80, Federal Republic of Germany
(Received 24 July 1990; revised manuscript received 28 September 1990)

Far-infrared reflectivity spectra of a 1.2 at. % In-doped $Pb_{0.75}Sn_{0.25}Te$ single crystal and galvanomagnetic data are presented. The infrared spectra were analyzed with use of a fitting procedure based on the plasmon-phonon interaction model. The plasma frequency was found to decrease at cooling from 300 to 30 K and a sharp drop in ω_p was observed between 20 and 10 K. In addition, at $T \leq 20$ K, a new structure on the reflectivity spectra is clearly observable. It may be associated with localized states in In-doped $Pb_{0.75}Sn_{0.25}Te$.

I. INTRODUCTION

$Pb_{1-x}Sn_xTe$ is a well-known narrow-band-gap semiconductor[1] with a usually very high ($n,p > 10^{17}$ cm^{-3}) intrinsic free-carrier concentration. Indium introduction into the $Pb_{1-x}Sn_xTe$ solid solution establishes an impurity level that is a function of the SnTe concentration and temperature.[2,3] For $0.28 > x > 0.22$ (dielectric states[2]), the In impurity level lies within the forbidden band and exhibits the attendant sharp drop in the free-carrier concentration. In their dielectric state, at temperatures below about 25 K, these In-doped alloys are unique in that they are photosensitive with a decrease in electrical resistivity of several orders of magnitude when illuminated by low-intensity infrared radiation.[4]

The nature of this persistent photoconductivity is not well understood. Three models have been put forward: (a) the impurity-autolocalized-state model,[5] (b) the Jahn-Teller center model,[6] and (c) the structural-phase-transition model.[7] It is a common feature that all three models postulate the existence of In impurity states. However none of the models explains a persistent photoconductivity mechanism in a satisfactory manner nor have they been tested conclusively experimentally.

Indium-doped $Pb_{1-x}Sn_xTe$ alloy optical and transport behavior has also attracted considerable interest in the past few years.[8-12] A $Pb_{1-x}Sn_xTe$(In) thin-film temperature-induced plasma-frequency shift has been observed,[8] a chemical-potential temperature dependence detected,[9] and a transport-property temperature and magnetic-field dependence has been found.[10] It has recently been shown that the band gaps do not change appreciably due to In doping, while the edge masses increase considerably as compared with those of undoped $Pb_{1-x}Sn_xTe$.[11] Moreover, a local vibrational mode has been observed at 160 cm^{-1} that is due to In local vibration in $Pb_{1-x}Sn_xTe$(In).[12]

In our earlier paper[13] we analyzed the far-infrared (FIR) spectra of the 0.5 at. % In-doped $Pb_{0.75}Sn_{0.25}Te$ single crystal and showed that if a photoinduced–free-carrier–concentration spatial distribution, is introduced into the plasmon-phonon interaction model, good agreement is obtained between experimental and theoretical spectra.

In this paper, we present 1.2 at. % In-doped $Pb_{0.75}Sn_{0.25}Te$ single-crystal far-infrared reflection spectra in the spectral range from 50 to 250 cm^{-1} at 10–300 K. These spectra were analyzed using a fitting procedure based on the plasmon-phonon interaction model. Below 20 K, a new structure was observed that has to be fitted by an additional oscillator and it may be explained in terms of $Pb_{0.75}Sn_{0.25}Te$(In) localized impurity states. Galvanomagnetic measurement data obtained on the same sample are also presented.

II. EXPERIMENTAL

The sample studied was an In-doped $Pb_{0.75}Sn_{0.25}Te$ single crystal grown by the modified Bridgeman method. The 1.2 at. % indium impurity was introduced into the liquid zone. The details of both the growth procedure and the measurement may be found in Ref. 13. A Bruker IFS 113v spectrometer was used to obtain 50- to 250-cm^{-1} far-infrared reflection spectra from 10 to 300 K.

III. RESULTS AND DISCUSSION

The 1.2 at. % In-doped $Pb_{0.75}Sn_{0.25}Te$ reflection spectra in the 50–250-cm^{-1} range from 300 to 10 K are given in Figs. 1(a)–1(g). Experimental data are depicted as

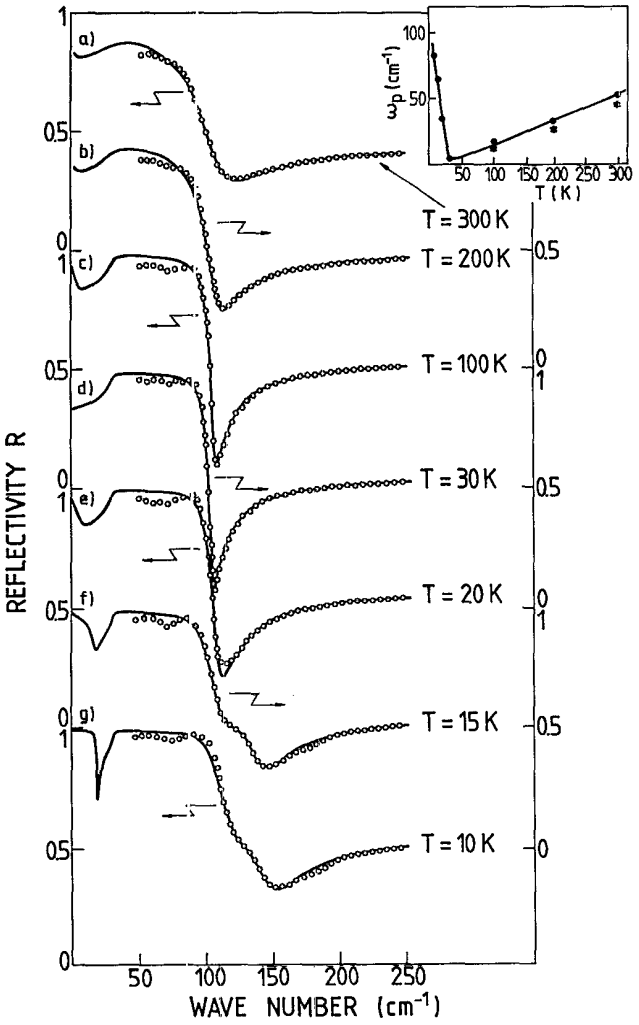

FIG. 1. Infrared reflection spectra of $Pb_{0.75}Sn_{0.25}Te(In)$ single crystal at seven temperatures. Experimental spectra are represented by circles. The solid lines are calculated spectra obtained by a fitting procedure based on the model given by Eqs. (1) and (2), with the parameter values given in Table I. Inset: Plasma-frequency temperature dependence of $Pb_{0.75}Sn_{0.25}Te(In)$. The circles and asterisk are ω_p values from Table I and from transport measurements, respectively. The solid line is a visual aid.

points. The lines were obtained using the plasmon-phonon interaction model

$$\epsilon(\omega)=\epsilon_\infty\left[1-\frac{\omega_p^2}{\omega(\omega+i\tau^{-1})}-\frac{\omega_{\mathrm{LO}}^2-\omega_{\mathrm{TO}}^2}{\omega_{\mathrm{TO}}^2-\omega^2-i\gamma_{\mathrm{TO}}\omega}\right], \quad (1)$$

where ω_{TO}, ω_{LO}, and ω_p are the transverse, longitudinal, and plasma frequency, respectively, γ_{TO} is the oscillator damping, τ the free-carrier relaxation time, and ϵ_∞ is the high-frequency dielectric constant. The first term in Eq. (1) is the free carrier and the second is the lattice vibration contribution to the dielectric constant. The spectra in Figs. 1(a)–1(d) were fitted using Eq. (1). As evidenced in these figures, the computed spectra and experimental data are in reasonably good agreement. The best fit parameters are listed in Table I. The reflectivity spectra were only observed down to 50 cm^{-1}. Thus the value of 32 cm^{-1} for ω_{TO} in Table I is from the literature.[8] As the temperature decreases toward 30 K, the plasma frequency and oscillator damping (Table I) decrease.

Due to plasmon–LO-phonon coupling, the LO-frequency assignment becomes uncertain. Thus, the reflectivity spectra depicted in Fig. 1(d) ($T=30$ K) were fitted first. At this temperature, the value of the resistivity of the illuminated sample [Fig. 2(a)] is at its highest, whereas the free-carrier concentration is very low ($n\cong 10^{13}$ cm^{-3}) shifting ω_p way below ω_{TO}, i.e., the plasmon and LO phonons decouple. The obtained $\omega_{\mathrm{LO}}=105$ cm^{-1} has been retained throughout the fitting of the other spectra in Fig. 1, i.e., its temperature dependence has been neglected. If this variation (usually of 1% over the 10–300-K range) is taken into account, the same fit as in Fig. 1(a) is obtained if ω_p is increased by not more than 4%. In the remainder of the cases depicted in Fig. 1 the inaccuracy of the ω_p determination is even smaller and as neglectible has no bearing on the discussion presented below. This particularly applies at temperatures below 30 K where a new structure emerges in a narrow temperature range over which the phonon mode temperature dependence has no effect.

At temperatures below 30 K, the reflection spectra change. First the plasma edge minimum widens [20 K, Fig. 1(e)], then a novel structure, a saddle hump, may be observed with a sharp shift of the plasma minimum to-

TABLE I. Optical parameters of phonons and plasmons (cm^{-1}) obtained by oscillator fitting of the $Pb_{0.75}Sn_{0.25}Te(In)$ reflection spectra.

	$T=300$ K	$T=200$ K	$T=100$ K	$T=30$ K	$T=20$ K	$T=15$ K	$T=10$ K
ω_p	52	34	20	5	35	65	82
τ^{-1}	100	33	10	3	11	8	1
ϵ_∞	30	39	50	52	58	58	58
ω_{TO1}	32	32	32	32	32	32	32
ω_{LO1}	105	105	105	105	105	105	105
γ_{TO1}	24	15	4	3	1	1	1
ω_{loc}					15.1	38.4	41.3
ω_0					115	124.2	130.1
G					35	44	49

wards the higher frequencies [Figs. 1(f) and 1(g)]. As a result an additional term appears in Eq. (1) (similarly as in Ref. 14):

$$\frac{\omega_{\text{loc}}^2}{\omega_0^2-\omega^2-i\omega G}\,, \tag{2}$$

where ω_0 is the characteristic frequency, G the damping, and ω_{loc}^2 the "strength" of the additional oscillator. As may be observed in 1(e)–1(g), the computed spectra obtained by means of Eqs. (1) and (2) agree well with experimental data. The thus obtained ω_p values are shown in the inset of Fig. 1. The obtained ω_p versus temperature dependence is in qualitatively agreement with the literature.[8,13] Namely, ω_p drops from 52 cm^{-1} (300 K) to 5 cm^{-1} (30 K) and then there is a sharp increase to 82 cm^{-1} (10 K). The increase in ω_p with the decrease in temperature below 30 K may be explained in terms of the persistent photoconductivity effect.

The resistivity versus temperature dependence for the same sample is given in Fig. 2(a). The line and dots are the unilluminated and low-intensity infrared radiation illuminated values, respectively. A dramatic difference in the illuminated and unilluminated $Pb_{0.75}Sn_{0.25}Te$(In) resistivity values may be observed only for $T<25$ K. This is due to the persistent photoconductivity effect. Electrical resistivity changes observed at $T<12$ K [Fig. 2(a)] are due to the nonlinearity of the voltage-current characteristic[15] of the system at these temperatures. The Hall constant (R_H) and free carrier concentration (n) temperature dependences for an unilluminated $Pb_{0.75}Sn_{0.25}Te$(In) sample are shown in Fig. 2(b). One can see the pronounced low-temperature activation part of $R_H(T)$. The corresponding activation energy obtained from $R_H \simeq \exp(E_a/2kT)$ (Ref. 16) is $\simeq 28$ meV.

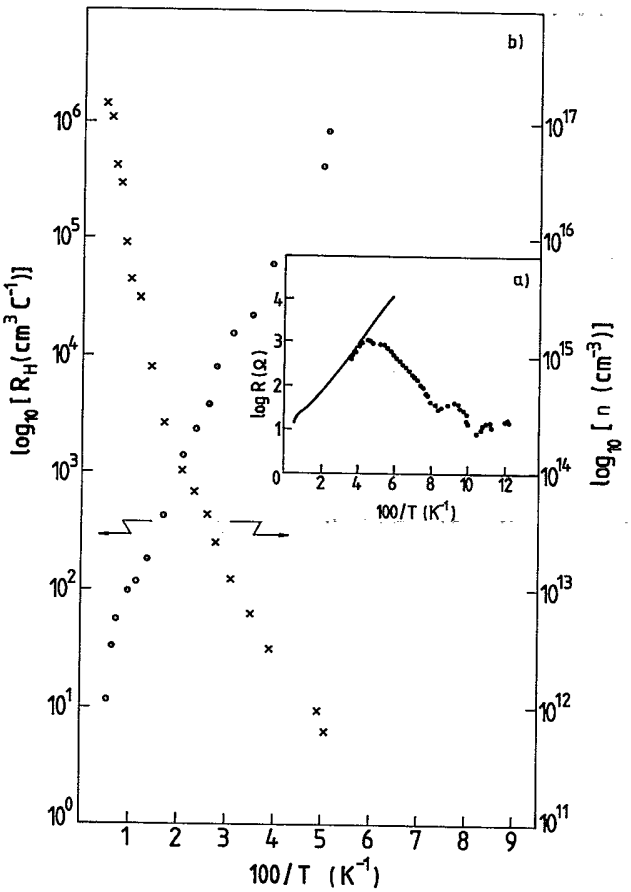

FIG. 2. $Pb_{0.75}Sn_{0.25}Te$(In) Hall coefficient (R_H) and free-carrier concentration (n) vs temperature. Inset: The resistivity vs temperature of the unilluminated (solid line) and illuminated (open circles) $Pb_{0.75}Sn_{0.25}Te$(In) single-crystal sample.

For the value of n taken in Fig. 2(b) of ϵ_∞ from Table I and the In-doped $Pb_{0.75}Sn_{0.25}Te$ m^*/m_0 temperature dependence from Ref. 13, we obtain the plasma frequency depicted by an asterisk in the inset of Fig. 1. As evidenced in the figure, the agreement of the optically and electrically determined ω_p values is relatively good.

Let us now return to Figs. 1(f) and 1(g), where the mentioned new structure (fitted by the additional oscillator) can easily be observed. A number of possible explanations may be put forward: (a) an In local vibrational mode, (b) a structural phase transition vibrational mode, (c) an In localized state related resonant electron oscillator. In our opinion, the 130-cm^{-1} mode at 10 K is not an In local vibration mode as it appears only at temperatures below 20 K, i.e., in the range of the persistent photoconductivity effect. In addition, the In local vibration mode of $Pb_{1-x}Sn_xTe$(In) may be observed[12] at 160 cm^{-1}, a value that is considerably higher than ω_0 (Table I). Moreover, the temperature dependence of this frequency is much stronger (1 cm^{-1}/K) than that usual for phonon vibrational modes (0.01 cm^{-1}/K). All this leads us to conclude that the 130-cm^{-1} mode is not a local In vibrational mode. The same applies to the assumption that it is due to a structural phase transition. Namely, it is claimed in Ref. 17 that $Pb_{1-x}Sn_xTe$ has a structural phase transition at $T\cong 20$ K from the cubic to the rhombohedral structure. If this were true, we would be justified in assuming that the 130-cm^{-1} mode is due to a reststrahlen peak of this new structure modification. This assumption is groundless because of the sharp ω_0 temperature dependence. Furthermore, the good fit for 1(f) to 1(g) is obtained if an oscillator at $\omega_{\text{TO}}=32$ cm^{-1} exists, whose damping decreases as the temperature drops (mode hardening, see Table I). We are led to conclude that the phase transition, if it exists, cannot be observed from the spectra presented in Fig. 1. The same applies to the results depicted in Fig. 2. Namely, neither the $R(T)$, nor the $R_H(T)$ dependence has a singularity at $T\cong 25$ K, indicating that a phase transition is not observable at these temperatures.

With all the above in mind, we conclude that the newly observed structure at $T\leq 20$ K is a persistent photoconductivity effect related, i.e., a result of localized In-level electron transitions as will be discussed further.

The temperature dependence of the additional oscillator parameters, obtained by the fitting of the observed spectra in Figs. 1(e)–1(g) in accordance with (1) and (2), is depicted in Fig. 3. The best fit values are given as an as-

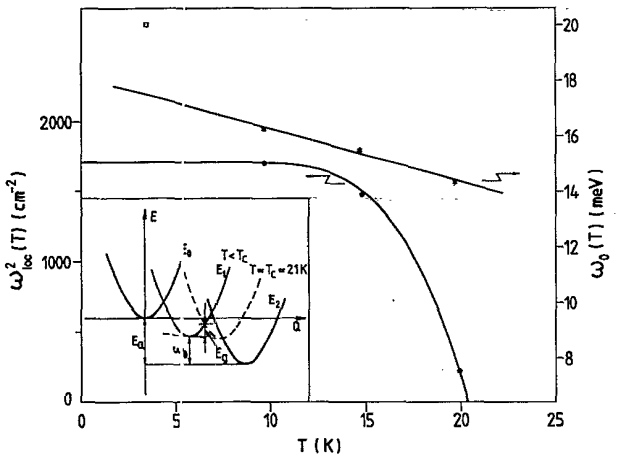

FIG. 3. Characteristic frequency (ω_0) and "strength" (ω_{loc}^2) temperature dependence of the additionally introduced oscillator. Inset: Configuration-coordinate diagram for indium in $Pb_{0.75}Sn_{0.25}Te$.

terisk, i.e., points for $\omega_0(T)$ and $\omega_{loc}^2(T)$, respectively. As shown in Fig. 3, the oscillator frequency (ω_0) temperature dependence is almost linear. The increase in ω_0 as the temperature is lowered is evident. The point (□) corresponds to an E_a activation energy obtained by low-temperature galvanomagnetic measurements[18] in the absence of infrared radiation. The linear extrapolation of $\omega_0(T)$ dependence yields a value somewhat lower than E_a at $T=4$ K.

The $\omega_{loc}^2(T)$ dependence is considerably more complex, it is exponential. A good fit (the line in Fig. 3) is obtained for

$$\omega_{loc}^2 = A\,[1-\exp(-E_g/kT)]\,, \tag{3}$$

where E_g is the two-electron to one-electron state barrier width (inset of Fig. 3). A linear E_g temperature dependence $E_g = B(T_c - T)$ results in a best fit parameter of $E_g(\text{meV}) = 0.52(21-T)$; $A = \omega_{loc}^2(0) = 1705.7$ cm^{-2}. Note that the $T_c = 21$ K value coincides with the persistent photoconductivity temperature obtained from galvanomagnetic measurements [Fig. 2(a)].

The three ω_{loc}^2 values shown in Fig. 3 are characteristic in that they lie at the limits of the $\omega_{loc}^2(T)$ dependence of $T=10$ and 20 K, i.e., at its greatest curvature ($T=15$ K). The shape of $\omega_{loc}^2(T)$ dependence has been confirmed by systematic reflectivity spectra measurements between 5 and 20 K.[19]

The additional oscillator is, in our opinion, related to the transition between E_2 localized two-electron states that stabilize the Fermi level and the E_1 metastable one-electron states. The existence of these states was detected both photoelectrically[20] and galvanomagnetically.[21]

The impurity center configuration state diagram is shown in the inset in Fig. 3. In accordance with $\omega_0(T)$ dependence, the energy of the minimum that corresponds to the one-electron state is near the bottom of the conduction band (state E_1 in the inset of Fig. 3). The E_1-state occupancy is strongly temperature dependent [$\omega_{loc}^2(T)$] indicating a change in the barrier width between E_1 and E_2. At $T=21$ K this barrier vanishes (the dashed line in the inset of Fig. 3) and its related ω_{loc} drops to zero. The coincidence of this temperature and the temperature of the onset of the persistent photoconductivity effect supports our assumption that persistent photoconductivity depends on nonequilibrium charge-carrier relaxation via the one-electron metastable localized state.

Persistent photoconductivity manifests itself in the ir spectra for $T<30$ K as a widening of the plasma minimum that in turn may be related to the nonuniform photoexcited charge-carrier distribution over the sample volume.[13] No significant widening may be observed in our sample. We are led to conclude that this effect is nonequilibrium photoexited charge carrier relaxation velocity related. Relaxation is considerably faster in $N_{In} \cong 1.2$ at.% than in $N_{In} \cong 0.5$ at.% samples,[22] the quasiequilibrium charge carrier concentration for the $N_{In} \cong 1.2$ at.% being considerably lower. This means that ω_p is smaller than ω_{LO}, the latter masking the plasma minimum.

IV. CONCLUSION

The measurements of far-infrared reflectivity spectra and of the galvanomagnetic coefficients were performed on an In-doped $Pb_{0.75}Sn_{0.25}Te$ single-crystal sample in the temperature range from 10 to 300 K. The persistent photoconductivity effect results in a substantial resistance decrease and plasma-edge shift at $T<25$ K. Moreover, at $T<20$ K a new structure in the reflectivity spectra of 1.2 at.% In-doped $Pb_{0.75}Sn_{0.25}Te$ is observed that may be explained in terms of a charge-carrier transition between localized two-electron and a metastable one-electron states.

[1]Yu. J. Ravich, B. A. Efimova, and J. A. Smirnov, in *Semiconducting Lead Chalogenides,* edited by L. S. Stilbius (Plenum, New York, 1970).

[2]B. A. Akimov, L. I. Ryabova, O. B. Yatsenko and S. M. Chudinov, Fiz. Tekh. Poluprovodn. **13**, 752 (1979) [Sov. Phys. Semicond. **13**, 441 (1979)].

[3]C. S. Lent, M. A. Bowen, R. S. Allgaier, J. D. Dow, O. F. Sankey, and E. S. Ho, Solid State Commun. **61**, 83 (1987).

[4]B. A. Akimov, N. B. Brandt, S. O. Klimonskiy, L. I. Ryabova, and D. R. Khokhlov, Phys. Lett. **88A**, 483 (1982).

[5]Yu. M. Kagan and K. A. Kikoin, Pis'ma Zh. Eksp. Teor. Fiz. **31**, 367 (1980)[[JETP Lett. **31**, 335 (1980)].

[6]B. A. Volkov and O. A. Pankratov, Dok. Akad. Nauk. SSSR **255**, 93 (1980) [Sov. Phys. Dokl. **25**, 922 (1980)].

[7]B. A. Volkov, V. V. Osipov, and O. A. Pankratov, Fiz. Tekh. Poluprovodn. **14**, 1387 (1980) [Sov. Phys. Semicond. **14**, 820 (1980)].

[8]S. W. McKnight and M. K. El-Rayess, Solid State Commun.

49, 1001 (1984).
[9]S. Takaoka, T. Itoga, and K. Murase, Jpn. J. Appl. Phys. **23**, 216 (1984).
[10]B. A. Akimov and N. B. Brandt, Physica **126B**, 361 (1984).
[11]S. Takaoka, S. Shimomura, H. Takahashi, and K. Murase, Phys. Rev. B **40**, 5642 (1989).
[12]S. Takaoka and K. Murase, J. Phys. Soc. Jpn. **52**, 25 (1983).
[13]N. Romčević, Z. V. Popović, D. R. Khokhlov, A. V. Nikorich, and W. Konig, Infrared Phys. (to be published).
[14]I. G. Neizvestnyi, Yu. A. Pusep, and M. P. Sinyukov, Fiz. Tverd. Tela (Leningrad) **28**, 3197 (1986) [Sov. Phys. Solid State **28**, 1802 (1986)].
[15]B. A. Akimov, N. B. Brandt, V. N. Nikiforov, Fiz. Tverd. Tela (Leningrad) **26**, 1602 (1984) [Sov. Phys. Solid State **26**, 973 (1984)].
[16]B. M. Vul, I. D. Voronova, G. M. Kalyuzhnaya, T. S. Mamedov, and T. Sh. Ragimova, Pis'ma Zh. Eksp. Teor. Fiz. **29**, 21 (1979) [JETP Lett. **29**, 18 (1979)].
[17]A. I. Belogorokhov, A. G. Belov, I. G. Neizvestnyi, Yu. A. Pusep, and M. P. Sinyukov, Zh. Eksp. Teor. Fiz. **92**, 869 (1987) [Sov. Phys. JETP **65**, 490 (1987)].
[18]B. A. Akimov, V. P. Zlomonov, L. I. Ryabova, O. B. Yatsenko, and S. M. Chudinov, Fiz. Tekh. Poluprovodn. **13**, 1239 (1979) [Sov. Phys. Semicond. **13**, 759 (1979)].
[19]N. Romčević, Z. V. Popović, and D. Khokhlov (unpublished).
[20]I. I. Zasavitskiy, A. B. Matveenko, B. N. Matsonashvili, and V. T. Trofimov, Fiz. Tekh. Poluprovodn. **21**, 1789 (1987) [Sov. Phys. Semicond. **21**, 1084 (1987)].
[21]B. A. Akimov, A. V. Nikorich, D. R. Khokhlov, and S. N. Chesnokov, Fiz. Tekh. Poluprovodn. **23**, 668 (1989) [Sov. Phys. Semicond. **23**, 418 (1989)].
[22]B. A. Akimov, A. V. Albul, H. V. Nikorich, L. I. Ryabova, and D. R. Khokhlov, Fiz. Tekh. Poluprovodn. **18**, 1778 (1984) [Sov. Phys. Semicond. **18**, 1112 (1984)].